Supplementary Information

Bacterial strains and plasmid construction

The partitioning operons from the following plasmids were synthesized by Epoch Life Sciences (www.epochlifescience.com): pCoo, CP-933T_UT, CP-933T, pKPN4, pADAP, pCP301, pAPEC. Both the R1, and R478 par operon was amplified directly from pKG503 (from Kenn Gerdes, University of Newcastle, UK) and R478 native plasmid (from Diane Taylor, University of Alberta, Canada) using primers oEMH1 + oEMH2, and oEMH53 + oEMH54 respectively. The pB171 Par operon was derived from pGE103 (1) (from Kenn Gerdes) and amplified using primers oEMH47 and oEMH48. The pSK41 Par operon, and the pCTX-M3 par operon were amplified from pSK9001 (2) and pJMB14 (3) respectively using primer pairs oEMH51 + oEMH52, and oEMH147 + oEMH148. pSK9001 and pJMB14 were provided by Neville Firth (University of Sydney, Australia) and Grazyna Jagura-Burdzy (Polish Academy of Sciences, Poland) respectively. All forward primers for amplification of homologous par sequences contained 20bp of identical sequence, and likewise for the reverse primers. This allowed the use of the same primer pair for subsequent cloning and manipulations (see below).

Plasmid pEMH606 was derived from a mini version of F1 plasmid, pDAG203 (4) provided by Jean-Ives Bouet (University of Toulouse, France) Initially the restriction sites SpeI and SacII were inserted into the pDAG302 plasmid upstream of the *ResD* ORF, by insertional PCR, simultaneously removing the *ccdA* and *ccdB** genes. The Lac promoter and LacZ gene were amplified from the *E. coli* chromosome using primers oEMH338 and EMH339, and the Lac terminator was amplified using primers oEMH340

+ oEMH341 respectively. Fusion PCR, was used to piece these fragments together to generate a LacZ gene that was inserted into pDAG203 at SpeI and SacII sites, creating pEMH606. To generate versions of pEMH606 containing the different partitioning operons, the restriction sites AflII and AvrII were synthetically inserted into pEMH606 using PCR, simultaneously removing the *rpl* gene. Partitioning operons were amplified with primers oEMH293 + oEMH294 containing AvrII and AflII sites, and ligated into pEMH606.

The challenge plasmids, series pEMH14x, where x is a number 0-13 are synthetic, and were constructed using ligation independent cloning (5) with four unique DNA molecules encoding 1. a Par operon, 2. the replication origin from plasmid pMB1(*oriMB1*), 3. the kanamycin resistance gene from pET28a (Merck, Darnstadt, Germany) and 4. green fluorescent protein (GFP) coding sequence optimized for expression in *E. coli*.

pB171 and pCP301 chimeric partitioning operons were assembled using fusion PCR, and amplified with oEMH293 and oEMH294 before cloning into pEMH606 at AflII and AvrII sites.

parC mKate reporter constructs (plasmid series pEMH700 to pEMH707) were generated by fusion PCR, whereby the gene encoding the red fluorescent protein, mKate, was amplified from the oriR1, Amp^R plasmid, pPM195 (provided by Per Malkus, Harvard Medical School), and both the *parC* promoters and 3‘UTRs of either pCP301 or pB171 par operons amplified from pEMH608 and pEMH617 respectively. Each reporter was amplified with primers oEMH498 and oEMH499 containing NheI and EagI restriction sites respectively, and cloned into pPM195 digested with the same enzymes.

The plasmid pPM70 was obtained from Per Malkus (Harvard Medical School) and contains the *ori* SC101-ts* (6), Amp^R gene, and RNA1 promoter driving expression of green fluorescent protein (GFP). This plasmid was used as the backbone to express Par proteins of both pB171 and pCP301 partitioning operons from this RNA1 promoter. Initially the GFP coding sequence was removed from pPM70 using restriction enzymes BamHI and XbaI. Next the required Par proteins were amplified with primers containing both these restriction sites, and ligated into the pPM70-digested backbone.

C-terminally His_6-tagged ParR expression plasmids were constructed by inserting either the pB171 ParR ORF or pCP301 ParR ORF at the BamHI and NotI sites of pET21a to create the plasmids pEMH535 and pEMH536. pB171 ParR was amplified with primers oEMH538 and oEMH540, and pCP301 ParR was amplified with primers oEMH539 and oEMH541. Table S2 summarizes the names and important features of all plasmids used in this study. All plasmid and primer sequences are available upon request.

Kinetic model of pB171 and pCP301 Partition Incompatibility

Since plasmid loss is a probabilistic process involving molecules present in very small numbers per cell, a stochastic approach is appropriate. We use first-order chemical kinetics to model association and dissociation between *parC* and ParR prior to cell division, simulating long enough so the final state samples from the steady state distribution, implemented using Gillespie's stochastic simulation algorithm The reactions modeled are:

(1)

$$C_{CP301} + R_{CP301} \underset{k_1^-}{\overset{k^+}{\rightleftharpoons}} C_{CP301}R_{CP301}$$

$$C_{CP301} + R_{B171} \underset{k_2^-}{\overset{k^+}{\rightleftharpoons}} C_{CP301}R_{B171} \quad (2)$$

$$C_{B171} + R_{CP301} \underset{k_3^-}{\overset{k^+}{\rightleftharpoons}} C_{B171}R_{CP301} \quad (3)$$

$$C_{B171} + R_{B171} \underset{k_4^-}{\overset{k^+}{\rightleftharpoons}} C_{B171}R_{B171}. \quad (4)$$

We include two kinds of plasmid, $C_{CP301} = parC_{pCP301}$, and $C_{B171} = parC_{pB171}$, and likewise two ParR binding proteins, R_{CP301} and R_{B171}. The model's *R* is a proxy for the complex of the number of ParR molecules that must bind a *parC* element to enable it to interact with and stabilize ParM filaments, rather than a single ParR. We take the binding constants k^+ to be identical, but the unbinding constants to be distinct for different pairs, leading to different steady-state binding probabilities. Modeling these reactions as first-order kinetics means that each reaction takes place at a rate given by the number (Equivalent to concentration as we model cell volume as fixed) of each ingredient present, multiplied by the reaction rate. For example if there are C_1 copies of plasmid 1 not bound to ParR, and R_A copies of ParR complexes not bound to plasmids, C_1R_A complexes are formed proportional to the number of free pairs: $k^+ [C_1] [R_A]$.

We take the total *parC* and ParR numbers per cell to be constant, so that production and degradation of ParR, and replication of *parC*, are excluded from the model. The total count of R complexes is fixed at 2x that of cognate *parC*; we performed simulations varying this ratio, and found no significant differences in loss rate as long as the total R complex count is greater than the *parC* count (Fig S7).

The initial state has all *parC*-ParR's unbound, and we run the simulation for 100x longer than the reciprocal of any of the rate constants, so that the final state retains no

memory of the initial conditions. For figure 4, we simulated 10,000 mother cells for each combination of parameters.

Due to the low diffusion rates of plasmids, the time for a plasmid at one end of the cell to diffuse away from that end is comparable to the generation time. Since filament extension is fast, 3 μm/min *in vitro* (7), we do not explicitly model filament formation, extension or dissociation. Instead we model segregation by assigning *parC*s to daughters probabilistically depending on their binding state. When we stop the simulation, unpaired *parC*'s are binomially distributed between daughters with equal probability. *parC*'s bound to ParR's of a given species are paired uniformly at random, and one plasmid from each pair assigned to each daughter; if there are an odd number then the last is assigned to one daughter at random.

Dissociation rates were estimated from the RFP binding assay in Figure S2, using the stochastic model of *parC*-ParR binding. Precisely, in the association-dissociation reaction:

$$C + R \underset{k^-}{\overset{k^+}{\rightleftharpoons}} CR \qquad (5)$$

assume the total number of *parC*'s present is fixed, comprised of free *parC*'s and those bound to ParR, $[C] + [CR]$. Then the proportion of *parC* unbound is:

$$p = \frac{[C]}{[C] + [CR]} \qquad (6)$$

At equilibrium,

$$k^+[C][R] = k^-[CR] \qquad (7)$$

where again [R] is the count of free ParR, so

$$\frac{k^-}{k^+[R]} = \frac{1-p}{p} \tag{8}$$

An estimate of the count of free ParR-complexes in the experimental conditions measured is thus necessary for an estimate of the (relative) reaction rates.

Utilizing RFP reporter constructs whose expression was driven by *parC* promoter sequences, we determined the level of fluorescence in the presence of constitutive amounts of ParR protein, since ParR binding to *parC* represses expression. This value, reported in figure S2, is a proxy for the proportion of ParR bound to *parC*. As we simulated with a 2x ratio of total ParR complexes to *parC*, for mathematical simplicity we approximated the count of free ParR complexes as equal to the *parC* copy number. In these experiments there were roughly 3-5 copies of *parC* present, so we approximate [R] total as 8 copies per cell. This approximation further assumes that the same R complex that mediates segregation is the single unit that mediates repression. The numerical values reported are in Table S3.

References

1. Ebersbach, G., and K. Gerdes. 2001. The double par locus of virulence factor pB171: DNA segregation is correlated with oscillation of ParA. Proc. Natl. Acad. Sci. U. S. A. **98:**15078-15083. doi: 10.1073/pnas.261569598.

2. **Schumacher, M. A., T. C. Glover, A. J. Brzoska, S. O. Jensen, T. D. Dunham, R. A. Skurray, and N. Firth.** 2007. Segrosome structure revealed by a complex of ParR with centromere DNA. Nature. **450:**1268-1271. doi: 10.1038/nature06392.

3. **Mierzejewska, J., A. Kulinska, and G. Jagura-Burdzy.** 2007. Functional analysis of replication and stability regions of broad-host-range conjugative plasmid CTX-M3 from the IncL/M incompatibility group. Plasmid. **57:**95-107. doi: 10.1016/j.plasmid.2006.09.001.

4. **Lemonnier, M., J. Y. Bouet, V. Libante, and D. Lane.** 2000. Disruption of the F plasmid partition complex in vivo by partition protein SopA. Mol. Microbiol. **38:**493-505.

5. **Aslanidis, C., and P. J. de Jong.** 1990. Ligation-independent cloning of PCR products (LIC-PCR). Nucleic Acids Res. **18:**6069-6074.

6. **Hamilton, C. M., M. Aldea, B. K. Washburn, P. Babitzke, and S. R. Kushner.** 1989. New method for generating deletions and gene replacements in Escherichia coli. J. Bacteriol. **171:**4617-4622.

7. **Garner, E. C., C. S. Campbell, and R. D. Mullins.** 2004. Dynamic instability in a DNA-segregating prokaryotic actin homolog. Science. **306:**1021-1025. doi: 10.1126/science.1101313.

Native Plasmid Name	Host Species	Native Plasmid Name	Host Species
R1	*Salmonella enterica*	pADAP	*Serratia entomophila*
pB171	*Escherichia coli*	pAPEC-O2-R	*Escherichia coli*
pCP301	*Shigella flexneri*	pCoo	*Escherichia coli*
pSK41	*Staphlacoccus aureus*	CP 933T_UT	*E. coli, UT 189/UPEC*
R478	*Serratia marcescens*	CP-933T	*E. coli, O157:H7*
pKPN4	*Klebsiella pneumoniae*	pCTX-M3	*Citrobacter freundi*

Table S1. The native plasmids and their bacterial hosts encoding the homologous Par operons utilized in this study.

Table S2: Plasmids used in this study.

Plasmid	Replicon (*ori*)	Drug Resistance Marker	Par Elements	Promoter driving Par Elements	Relevant Figure	Source
pEMH606	F1	Cm^R	-	-	Figure 1c	This study
pEMH607	F1	Cm^R	R1 ParMRC	R1 Par	Figure 1c	This study
pEMH608	F1	Cm^R	pCP301 ParMRC	pCP301 Par	Figure 2b	This study
pEMH617	F1	Cm^R	pB171 ParMRC	pB171 Par	Figure 2b	This study
pEMH515	F1	Cm^R	R478 ParMRC	R478 Par	Figure 2b	This study
pEMH516	F1	Cm^R	pCP301 ParMRC	pCP301 Par	Figure 2b	This study
pEMH517	F1	Cm^R	pADAP ParMRC	pADAP Par	Figure 2b	This study
pEMH518	F1	Cm^R	CP-933T ParMRC	CP-933T Par	Figure 2b	This study
pEMH519	F1	Cm^R	pCoo ParMRC	pCoo Par	Figure 2b	This study
pEMH520	F1	Cm^R	pKPN4 ParMRC	pKPN4 Par	Figure 2b	This study
pEMH521	F1	Cm^R	pCT-MX3 ParMRC	pCT-MX3 Par	Figure 2b	This study
pEMH522	F1	Cm^R	pAPEC ParMRC	pAPEC Par	Figure 2b	This study
pEMH523	F1	Cm^R	pSK41 ParMRC	pSK41 Par	Figure 2b	This study
pEMH524	F1	Cm^R	CP-933T_UT ParMRC	CP-933T_UT Par	Figure 2b	This study
pEMH140	pMB1	Kan^R	-	-	Figure 1c	This study
pEMH141	pMB1	Kan^R	R1 ParMRC	R1 Par	Figure 1c	This study
pEMH142	pMB1	Kan^R	pSK41 ParMRC	pSK41 Par	Figure 2b	This study
pEMH143	pMB1	Kan^R	pB171 ParMRC	pB171 Par	Figure 2b	This study
pEMH144	pMB1	Kan^R	R478 ParMRC	R478 Par	Figure 2b	This study
pEMH146	pMB1	Kan^R	pCT-MX3 ParMRC	pCT-MX3 Par	Figure 2b	This study
pEMH147	pMB1	Kan^R	pCP301 ParMRC	pCP301 Par	Figure 2b	This study
pEMH149	pMB1	Kan^R	pADAP ParMRC	pADAP Par	Figure 2b	This study
pEMH1410	pMB1	Kan^R	pKPN4 ParMRC	pKPN4 Par	Figure 2b	This study
pEMH1413	pMB1	Kan^R	CP-933T_UT ParMRC	CP-933T_UT Par	Figure 2b	This study
pEMH627	F1	Cm^R	C(301)R(301)M(171)	pCP301 Par	Figure 3a	This study
pEMH624	F1	Cm^R	C(301)R(171)M(301)	pCP301 Par	Figure 3a	This study
pEMH633	F1	Cm^R	C(171)R(301)M(301)	pCP301 Par	Figure 3a	This study
pEMH625	F1	Cm^R	C(171)R(171)M(301)	pB171 Par	Figure 3a	This study
pEMH623	F1	Cm^R	C(171)R(301)M(171)	pB171 Par	Figure 3a	This study
pEMH632	F1	Cm^R	C(171)R(301)M(171)	pB171 Par	Figure 3a	This study
pEMH531	F1	Cm^R	pCP301 *parC*	-	Figure 3b	This study
pPM70	SC101-ts*	Amp^R	-	-	Figure 3b	Per Malkus
pEMH611	SC101-ts*	Amp^R	pB171 ParRM	RNA1pr_1%**	Figure 3b	This study
pEMH640	pMB1	Kan^R	pCP301 *parC*	-	Figure 5a	This study
pEMH639	pMB1	Kan^R	pB171 *parC*	-	Figure 5a	This study
pEMH644	SC101-ts*	Amp^R	pCP301 ParR	RNA1pr_1%	Figure 5b	This study
pEMH645	SC101-ts*	Amp^R	pB171 ParR	RNA1pr_1%	Figure 5b	This study
pTRG	ColE1	Tet^R	-	-	Figure S2/S4	Agilent Technologies
pEMH653	ColE1	Tet^R	pCP301 ParR	RNA1pr_100%‡	Figure S4	This study
pEMH654	ColE1	Tet^R	pB171 ParR	RNA1pr_1%	Figure S2/S4	This study
pEMH655	ColE1	Tet^R	pCP301 ParR	RNA1pr_1%	Figure S2/S4	This study
pEMH656	ColE1	Tet^R	pB171 ParR	RNA1pr_100%	Figure S4	This study
	* = temperature sensitive SC101 *ori*, stable at <30°C (Hamilton et al. 1989)					
	** = Mutant form of RNA1 promoter with relative expression strength ~ 1%					
	‡ = Non-mutant RNA1 promoter with relative expression strength ~ 100%					

Plasmid	Replicon (*ori*)	Drug Resistance Marker	Reporter Construct	Relevant Figure	Source
pEMH700	R1	Amp^R	pCP301 *parC*, mKate, pCP301 ParR, pCP301 3'UTR	Figure 3c	This study
pEMH701	R1	Amp^R	pCP301 *parC*, mKate, pCP301 3'UTR	Figure 3c	This study
pEMH702	R1	Amp^R	pCP301 *parC*, mKate, pB171 ParR, pCP301 3'UTR	Figure 3c	This study
pEMH703	R1	Amp^R	pCP301 *parC*, mKate, pB171 ParR_K6E, pCP301 3'UTR	Figure 3c	This study
pEMH704	R1	Amp^R	pB171 *parC*, mKate, pB171 ParR, pB171	Figure 3c	This study

			3‘UTR		
pEMH705	R1	Amp^R	pB171 *parC*, mKate, pB171 ParR_K6E, pB171 3‘UTR	Figure 3c	This study
pEMH706	R1	Amp^R	pB171 *parC*, mKate, pB171 3‘UTR	Figure 3c	This study
pEMH707	R1	Amp^R	pB171 *parC*, mKate, pCP301 ParR, pB171 3‘UTR	Figure 3c	This study

Parameter	*parC*-ParR identity	p(unbound)	$k^-/k^+[R]$
k_1^-	$parC_{CP301}$ - $ParR_{CP301}$	9.60%	0.11
k_2^-	$parC_{CP301}$ - $ParR_{B171}$	32.60%	0.48
k_3^-	$parC_{B171}$ - $ParR_{CP301}$	82%	1.86
k_4^-	$parC_{B171}$ - $ParR_{B171}$	14.60%	0.17

Table S3: Parameters used for plasmid segregation simulations.

Since we only have relative estimates of k^-/k^+, in our simulation units of time were defined so that the association rate $k^+ = 1$, and the other parameters were scaled accordingly.

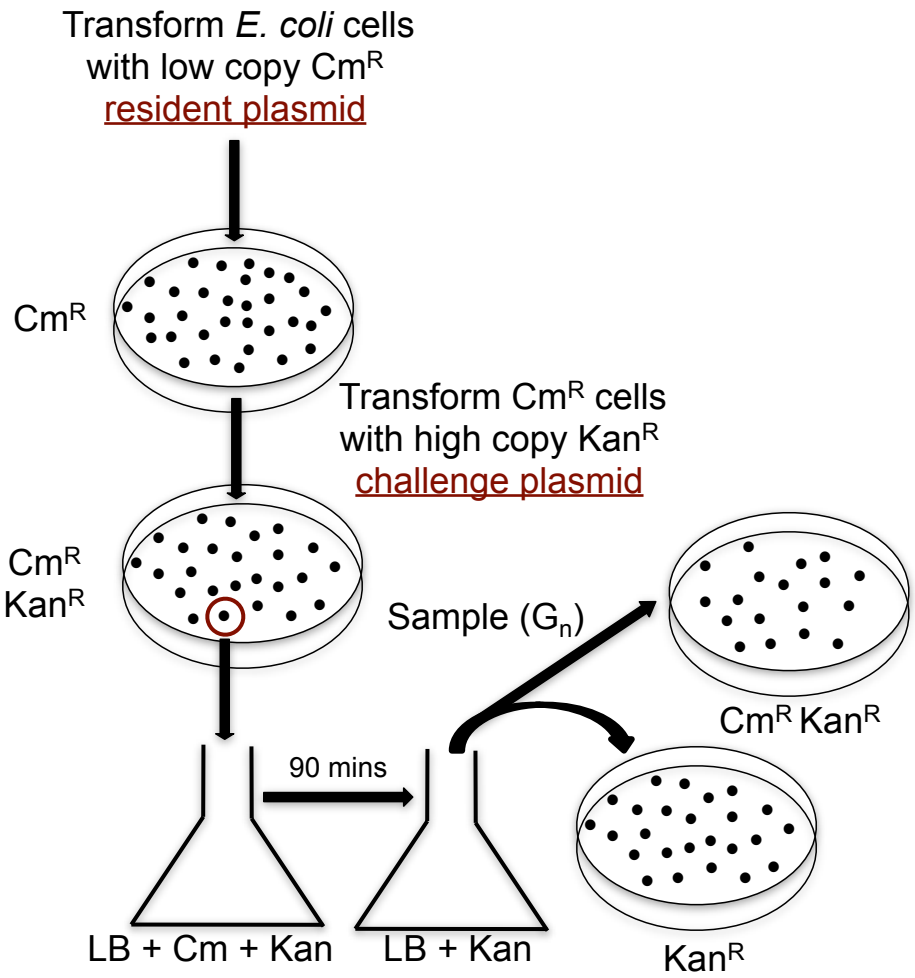

Figure S1. Plasmid incompatibility assay. Schematic of the plasmid compatibility assay undertaken in the study. Initially DH5alpha cells are transformed with the low copy chloramphenicol resistant (Cm^R) resident plasmid. Transformants are then transformed with the higher copy kanamycin resistant (Kan^R) challenge plasmid and transformants are selected on LB plates containing both chloramphenicol and kanamycin. A single colony is then grown for 90mins in the presence of both drugs, transferred to media containing only kanamycin to select for the challenge plasmid, and grown for approximately 70 generations. At various intervals during this time, the population is sampled and plated on media containing kanamycin alone or kanamycin and chloramphenicol. The fraction of doubly resistant colonies (Cm^RKan^R) to Kan^R colonies is determined and the loss rate of the Cm^R resident plasmid is determined.

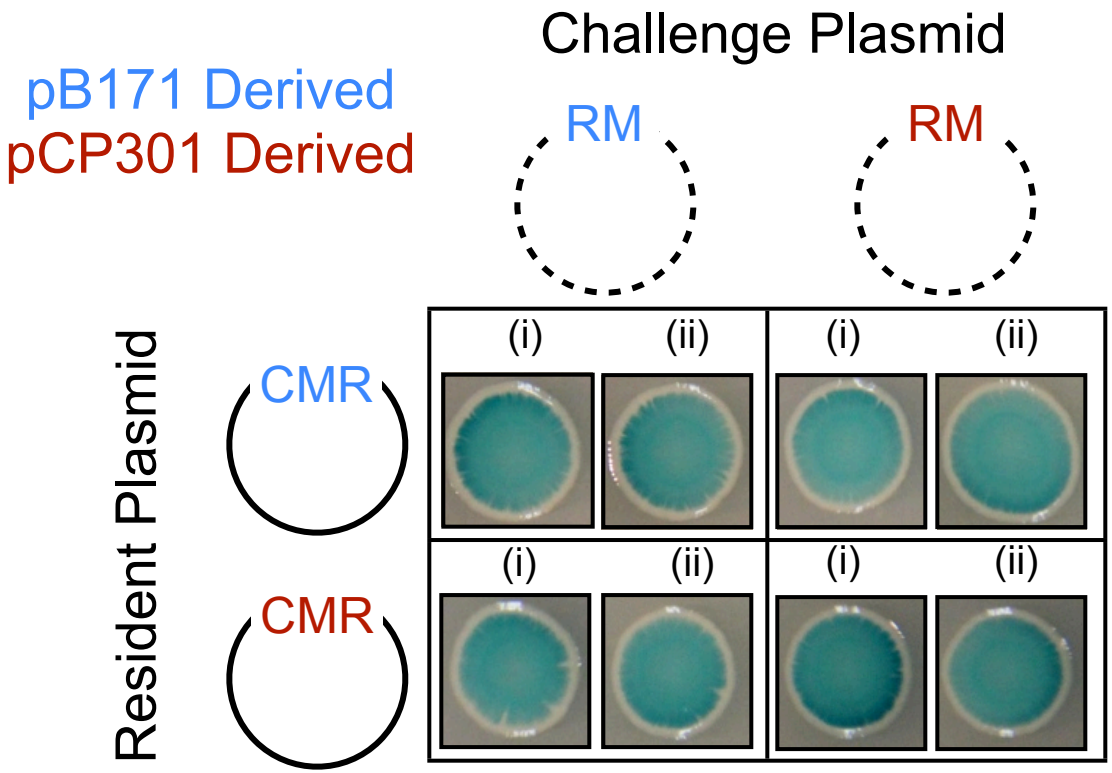

Figure S2. The requirement of *parC* sequence to mediate incompatibility. Qualitative plasmid incompatibility assay for strains containing the indicated plasmids, showing that the resident plasmid was not lost for all combinations tested. (i) an (ii) denote two independent transformants of the same strain for comparison.

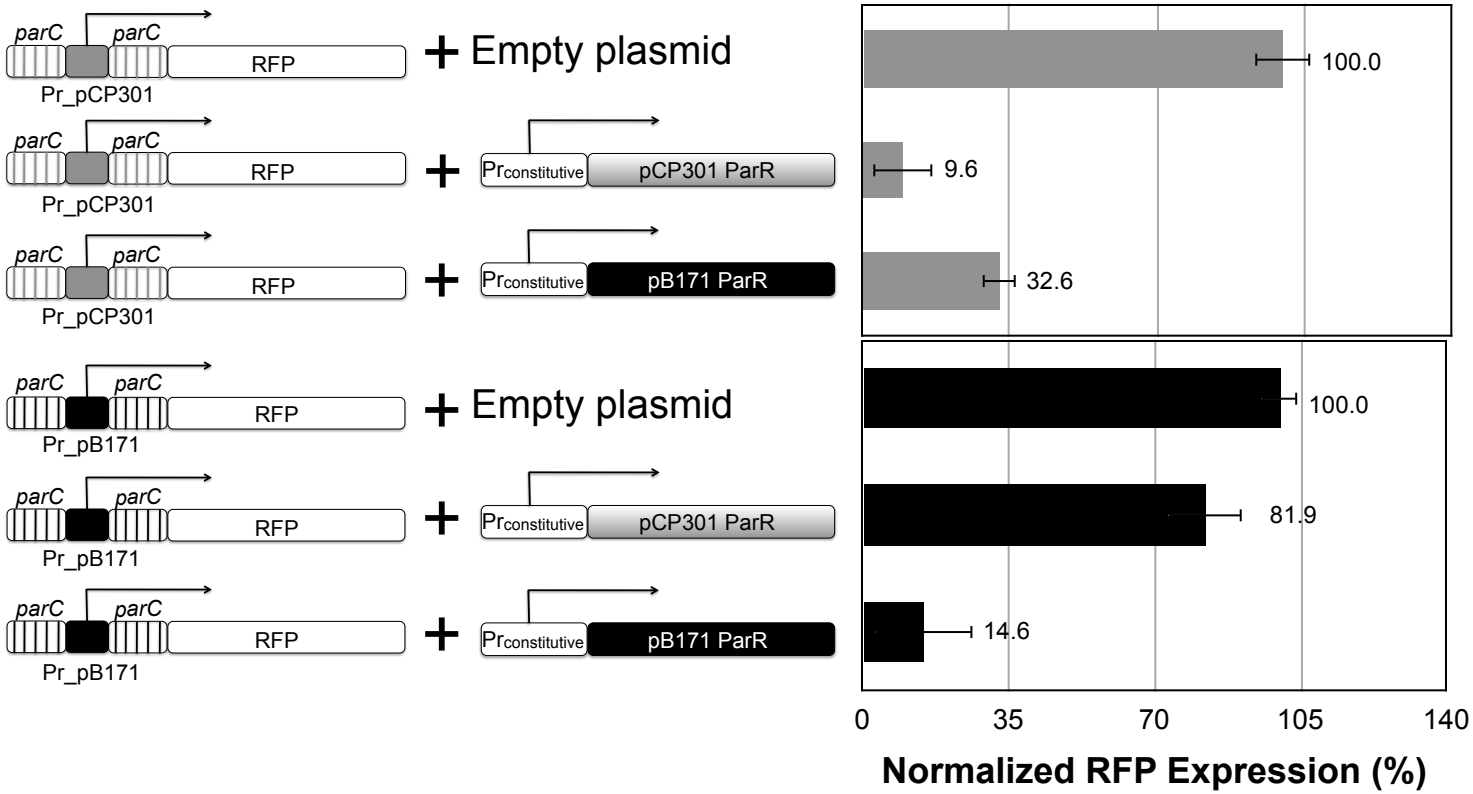

Figure S3. The binding of ParR proteins to *parC* DNA *in trans*. RFP fluorescence reporter assay for cells containing either the RFP gene expressed from the pCP301 promoter (Pr_pCP301) or pB171 promoter (Pr_pB171), in addition to a second plasmid encoding either $ParR_{pCP301}$, or $ParR_{pB171}$ from a constitutive promoter (RNA1 promoter). An empty plasmid control is used to normalize all fluorescence data. . Data represents the mean fluorescence, as determined by flow cytometry, of each strain. Error bars represent the standard deviation derived from six independent transformants of both the reporter plasmids and the ParR expressing plasmids.

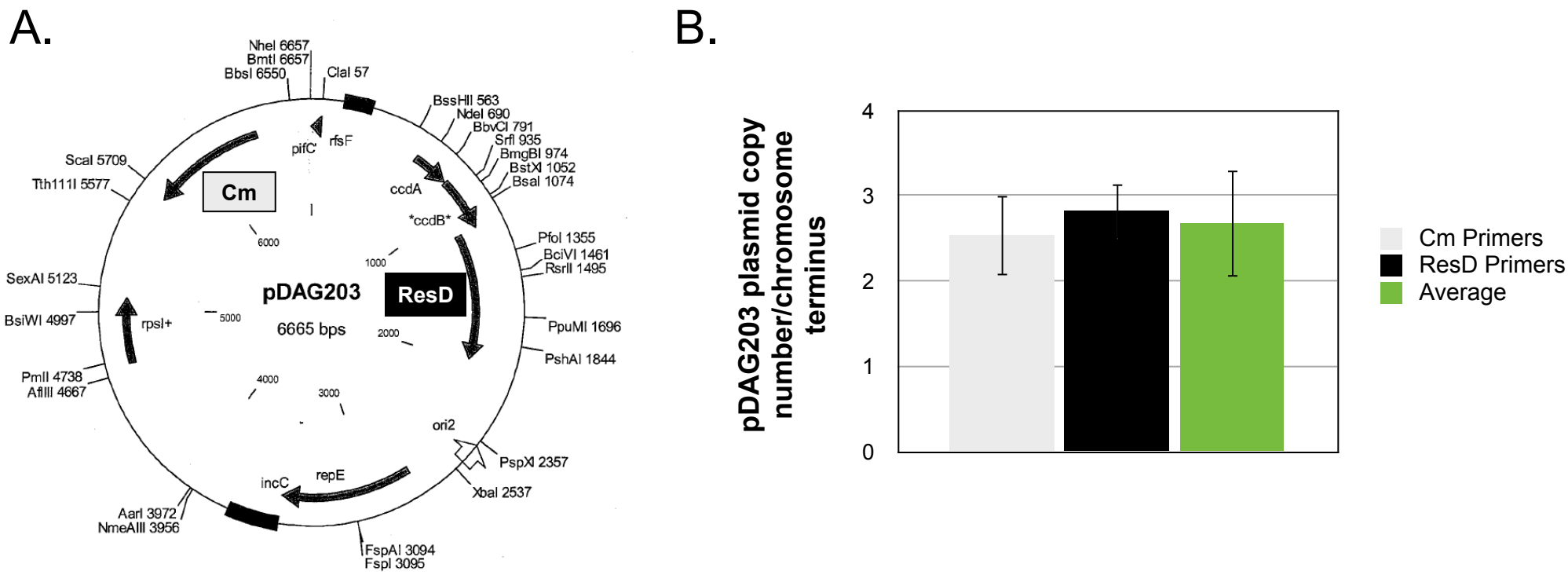

Figure S4. Copy number determination of oriF1 pDAG203 plasmid. A. Plasmid map of pDAG203 indicating the positions of the chloramphenicol (Cm) gene and resolvase (ResD) gene. **B.** Quantitative PCR analysis of DNA extracted from cells harboring pDAG203 using two primer pairs amplifying either the Cm or ResD genes.

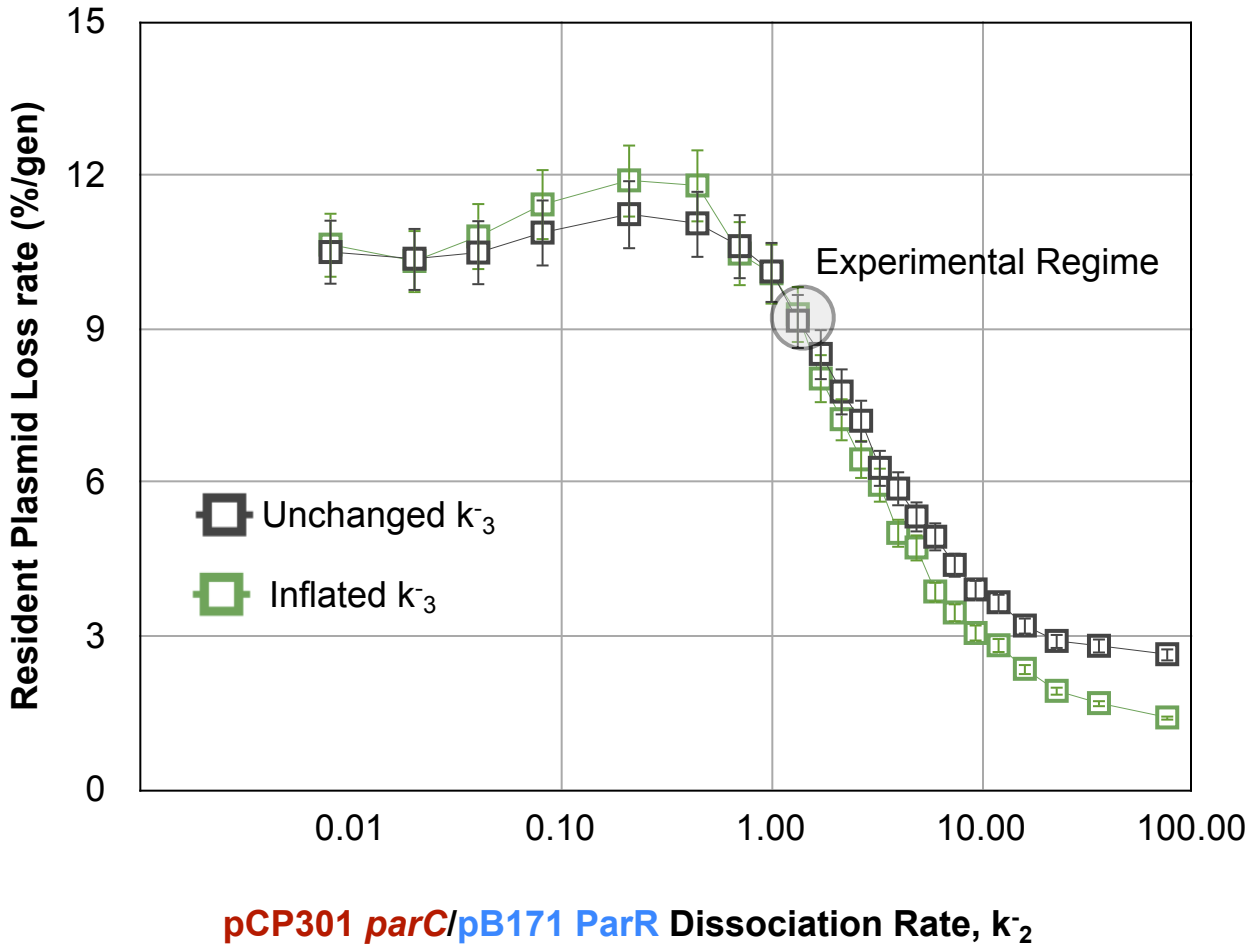

Figure S5. The incompatibility between a resident Par_{pCP301} plasmid, and Par_{pB171} challenge plasmid was simulated by our kinetic model under a range of values for k^{-}_{2} (the dissociation rate of $ParR_{pB171}$ binding to $parC_{pCP301}$) to determine the dependence of our model on k^{-}_{2}. The contribution of the dissociation rate of $ParR_{pCP301}$ binding to $parC_{pB171}$ (rate k^{-}_{3}), to resident plasmid loss rate was also monitored by inflating the value of k^{-}_{3} to a highly unfavorable value. In all simulations for this panel, resident and challenge plasmid copy numbers were set at 3 and 15 respectively. The experimentally determined value for k^{-}_{2} is highlighted for comparison. Error bars represent the 95% confidence interval.

A. *parC* sequence alignment:

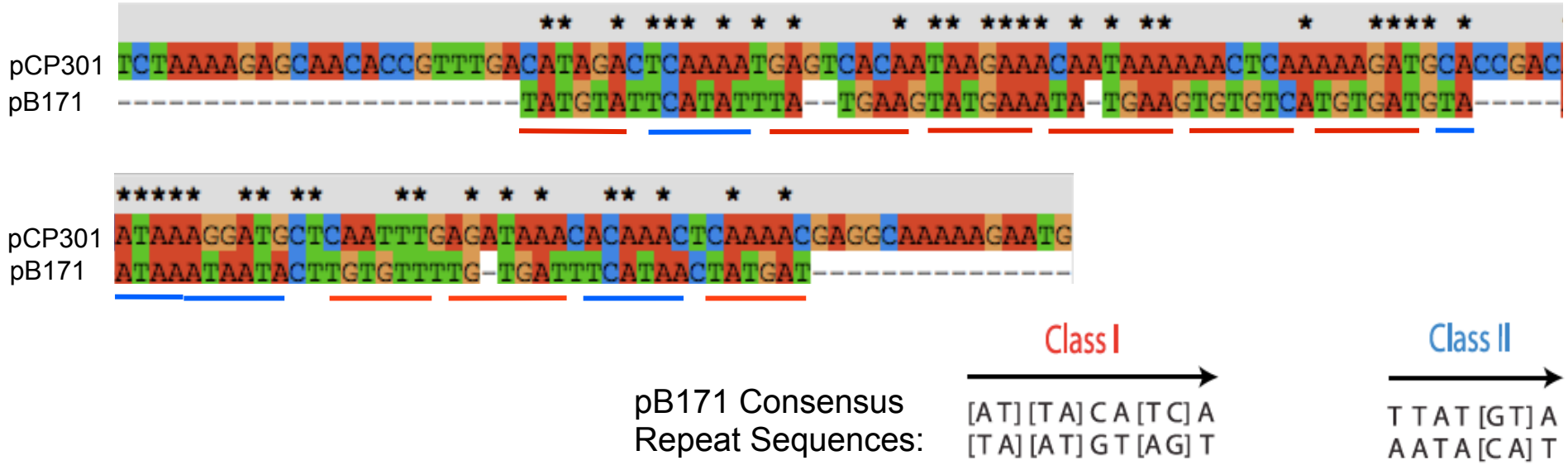

B.

ParR N-terminus sequence alignment:

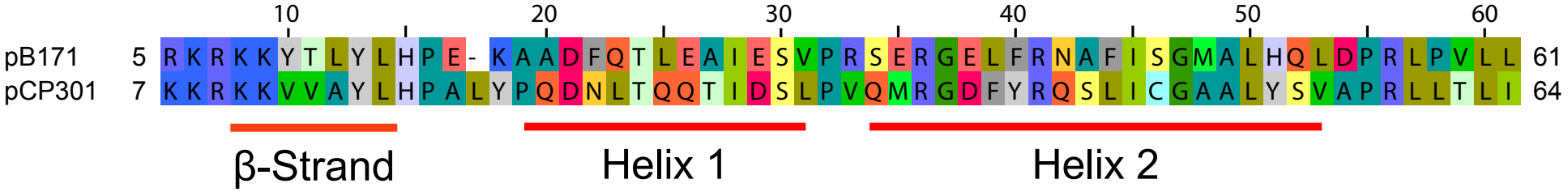

Figure S6. Sequence comparisons of pB171 and pCP301 *parC* and ParR. A. The *parC* sequence from both pB171 and pCP301 par operons were aligned using CLUSTALW. (* = identical bases between both sequences). The pB171 consensus repeat sequences, as determined by Ringgard, S. *et al* 2007 are also shown, and the relevant sequences are underlined in the alignment in either red, to denote the class1 consensus sequence, or in blue, to denote the class II consensus sequence. **B.** Alignment of the N terminal portions of ParR from pB171 and pCP301. Amino acids are colored according to their chemical properties and the regions that form the β-strand, Helix 1 and Helix 2, which comprise the DNA-interacting interface are underlined.

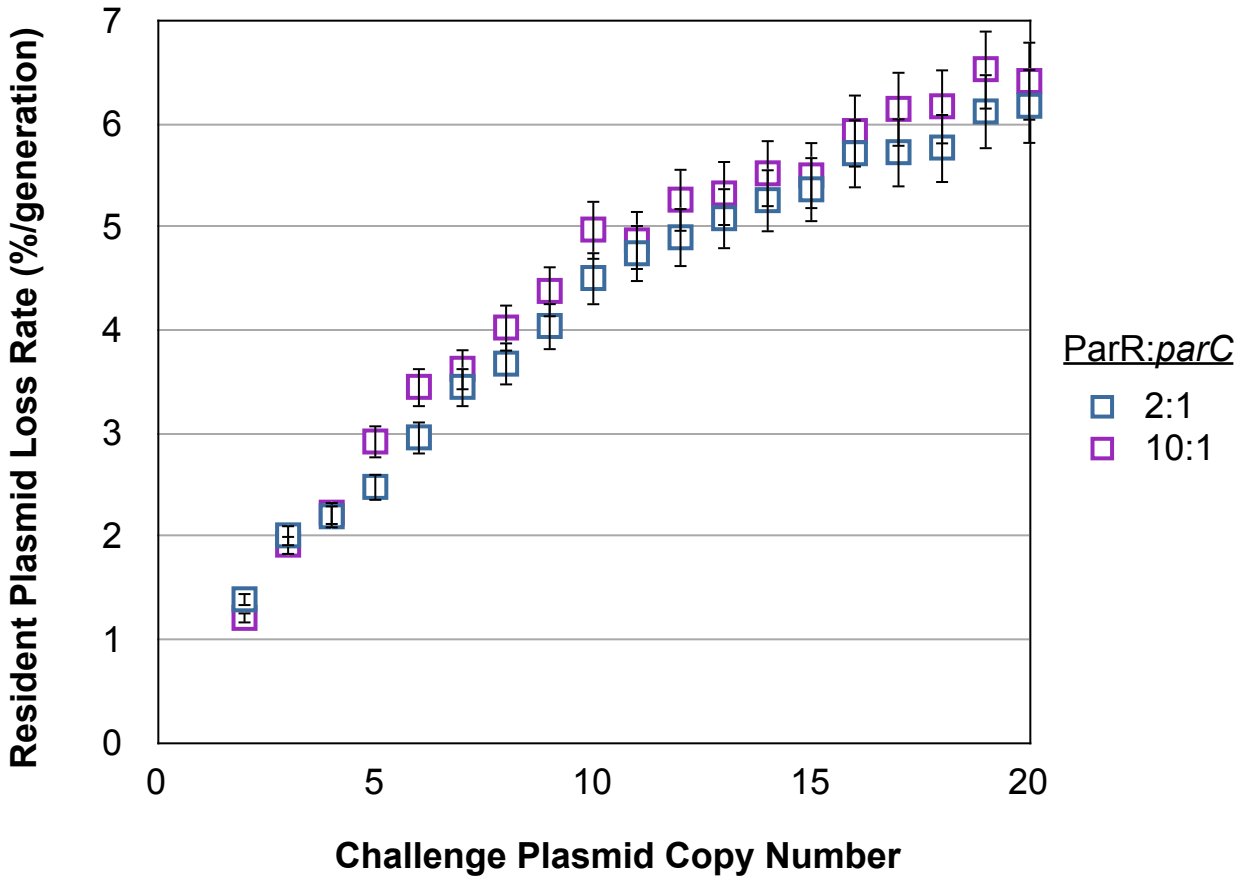

Figure S7. The incompatibility between a resident Par_{pCP301} plasmid, and Par_{pB171} challenge plasmid was simulated by our kinetic model under a range of values for the copy number of the Par_{pB171} challenge plasmid. The sensitivity of our model to the ratio between ParR complexes and *parC* DNA of both resident and challenge plasmids was tested by comparing the loss rates of the resident plasmid under two regimes, where this ratio was either 2:1 or 10:1. p_unbound values are as follows: k^{-}_{1} =3.0%, k^{-}_{2} =38.5%, k^{-}_{3} =55.2%, and k^{-}_{4} =47.2% Data indicate that there is no significant difference between these two situations. Error bars represent the 95% confidence interval.